

The dynamics of Plutinos

Qingjuan Yu and Scott Tremaine
 Princeton University Observatory, Peyton Hall,
 Princeton, NJ 08544-1001, USA

ABSTRACT

Plutinos are Kuiper-belt objects that share the 3:2 Neptune resonance with Pluto. The long-term stability of Plutino orbits depends on their eccentricity. Plutinos with eccentricities close to Pluto (fractional eccentricity difference $\Delta e/e_p = |e - e_p|/e_p \lesssim 0.1$) can be stable because the longitude difference librates, in a manner similar to the tadpole and horseshoe libration in coorbital satellites. Plutinos with $\Delta e/e_p \gtrsim 0.3$ can also be stable; the longitude difference circulates and close encounters are possible, but the effects of Pluto are weak because the encounter velocity is high. Orbits with intermediate eccentricity differences are likely to be unstable over the age of the solar system, in the sense that encounters with Pluto drive them out of the 3:2 Neptune resonance and thus into close encounters with Neptune. This mechanism may be a source of Jupiter-family comets.

Subject headings: planets and satellites: Pluto — Kuiper Belt, Oort cloud — celestial mechanics, stellar dynamics

1. Introduction

The orbit of Pluto has a number of unusual features. It has the highest eccentricity ($e_p = 0.253$) and inclination ($i_p = 17.1^\circ$) of any planet in the solar system. It crosses Neptune's orbit and hence is susceptible to strong perturbations during close encounters with that planet. However, close encounters do not occur because Pluto is locked into a 3:2 orbital resonance with Neptune, which ensures that conjunctions occur near Pluto's aphelion (Cohen & Hubbard 1965). More precisely, the critical argument $3\lambda_p - 2\lambda_n - \varpi_p$ librates around 180° with a period of 1.99×10^4 yr and an amplitude of 82° ; here λ_p and λ_n are the mean longitudes of Pluto and Neptune and ϖ_p is Pluto's longitude of perihelion. Other resonances are present with longer periods: for example, Pluto's argument of perihelion librates with an amplitude of 23° and a period of 3.8 Myr. In part because of its rich set

of resonances, Pluto’s orbit is chaotic, although it exhibits no large-scale irregular behavior over Gyr timescales (see Malhotra & Williams 1997 for a comprehensive review of Pluto’s orbit). For reference, Pluto’s semimajor axis and orbital period are $a_p = 39.774$ AU and $P_p = 250.85$ yr.

The most compelling explanation for Pluto’s remarkable orbit was given by Malhotra (1993, 1995). Malhotra argues that Pluto formed in a low-eccentricity, low-inclination orbit in the protoplanetary disk beyond Neptune. Subsequent gravitational scattering and ejection of planetesimals in the disk by all four giant planets caused Neptune’s orbit to migrate outwards (Fernández & Ip 1984). As its orbit expands, Neptune’s orbital resonances sweep through the disk, first capturing Pluto into the 3:2 resonance and then pumping up its eccentricity. If Pluto’s orbit was circular before capture, its present eccentricity implies that it was captured when Neptune’s semimajor axis was 0.814 times its current value or 24.6 AU (eq. 5). This process may also excite Pluto’s inclination although the details are less certain (Malhotra 1998).

Malhotra’s argument predicts that most Kuiper belt objects with $30 \text{ AU} \lesssim a \lesssim 50 \text{ AU}$ should also be captured—and presently located—in Neptune resonances (Malhotra 1995). This prediction has proved to be correct: of the ~ 90 Kuiper belt objects with reliable orbits as of 1999 January 1, over 30% have semimajor axes within 1% of the 3:2 resonance (although this number is exaggerated by observational selection effects). These objects have come to be called Plutinos, since they share the 3:2 resonance with Pluto (see Malhotra et al. 1999 for a recent review of the Kuiper belt).

Almost all studies of the dynamics of the Kuiper belt so far have neglected the gravitational influence of Pluto, because of its small mass ($M_p/M_\odot = 7.40 \times 10^{-9}$ for the Pluto-Charon system, Stern 1992, Tholen & Buie 1997). However, like the Trojan asteroids and Jupiter, or the Saturn coorbital satellites Janus and Epimetheus, Pluto and the Plutinos share a common semimajor axis and hence even the weak gravitational force from Pluto can have a substantial influence on the longitude of a Plutino relative to Pluto. A crude illustration of the importance of Pluto’s gravity is to note that the half-width of the 3:2 resonance, $(\Delta a/a)_{\text{res}} \simeq 0.01$ for $0.2 \lesssim e \lesssim 0.3$ (the maximum fractional amplitude of stable libration in semi-major axis, Malhotra 1996), is only a few times larger than the Hill radius of Pluto, $(\Delta a/a)_{\text{H}} = (M_p/3M_\odot)^{1/3} = 0.0014$.

The goal of this paper is to explore the dynamical interactions between Pluto and Plutinos and their consequences for the present structure of the Kuiper belt. Section 2 provides an approximate analytical description of the interactions, §3 describes the results of numerical orbit integrations, and §4 contains a discussion.

2. Analysis

We examine a simplified model solar system containing only the Sun and Neptune, with masses M_\odot and M_n ; we assume that Neptune’s orbit is circular and neglect all orbital inclinations. We describe the motion of the Plutino using the canonical variables

$$\begin{aligned} x_1 &= (GM_\odot a)^{1/2}, & y_1 &= \lambda, \\ x_2 &= (GM_\odot a)^{1/2}[1 - (1 - e^2)^{1/2}], & y_2 &= -\varpi, \end{aligned} \quad (1)$$

where a and e are the semi-major axis and eccentricity, λ and ϖ are the mean longitude and longitude of perihelion. The same variables for Neptune or Pluto are denoted by adding a subscript “n” or “p”.

We consider only the resonant perturbations exerted by Neptune, which can only depend on angles as an even function of the combination $3y_1 - 2y_{n1} + y_2$. Thus the Hamiltonian of a Plutino may be written

$$H_0(\mathbf{x}, \mathbf{y}, t) = H_K(x_1) + A(\mathbf{x}, 3y_1 - 2y_{n1} + y_2) + B(\mathbf{x}, \mathbf{y}, t), \quad (2)$$

where $H_K(x_1) = -\frac{1}{2}(GM_\odot)^2/x_1^2$ is the Kepler Hamiltonian, A is the resonant potential from Neptune, and $B(\mathbf{x}, \mathbf{y}, t)$ is the potential from Pluto. The same Hamiltonian describes the motion of Pluto if we set $B = 0$.

Now impose a canonical transformation to new variables (\mathbf{J}, \mathbf{w}) defined by the generating function

$$S(\mathbf{J}, \mathbf{y}, t) = J_1(3y_1 - 2y_{n1} + y_2) + \frac{1}{3}J_2(y_2 - y_{p2}). \quad (3)$$

Thus $w_1 = \partial S/\partial J_1 = 3y_1 - 2y_{n1} + y_2$, $w_2 = \partial S/\partial J_2 = \frac{1}{3}(y_2 - y_{p2})$, while $x_1 = \partial S/\partial y_1 = 3J_1$, $x_2 = \partial S/\partial y_2 = J_1 + \frac{1}{3}J_2$, and the new Hamiltonian is

$$H(\mathbf{J}, \mathbf{w}, t) = H_0 + \frac{\partial S}{\partial t} = H_K(3J_1) - 2\dot{y}_{n1}J_1 - \frac{1}{3}\dot{y}_{p2}J_2 + A(3J_1, J_1 + \frac{1}{3}J_2, w_1) + B, \quad (4)$$

where \dot{y}_{n1} is the mean motion of Neptune and $-\dot{y}_{p2}$ is the apsidal precession rate of Pluto.

To proceed further we make use of the fact that $B/A = O(M_p/M_n) \ll 1$. Thus we can divide the motion of a Plutino into “fast” and “slow” parts. The fast motion is determined by the Kepler Hamiltonian H_K and the resonant potential A (this is the opposite of normal usage, where the resonant perturbations from Neptune are regarded as “slow” compared to non-resonant perturbations). The slow variations are caused by the Pluto potential B .

First we examine the fast motion. We drop the potential B , so that w_2 is ignorable and $J_2 = 3x_2 - x_1 = (GM_\odot a)^{1/2}[2 - 3(1 - e^2)^{1/2}]$ is a constant of the motion. Thus if Pluto was

captured into resonance from a circular orbit with semimajor axis a_i , its present semimajor axis and eccentricity are related by

$$e^2 = \frac{5}{9} - \frac{4}{9}(a_i/a)^{1/2} - \frac{1}{9}(a_i/a). \quad (5)$$

We write $J_1 = J_{1r} + \Delta J_1$ where J_{1r} is chosen to satisfy the resonance condition for the Kepler Hamiltonian,

$$2\dot{y}_{n1} = 3\dot{y}_1 = 3\frac{dH_K}{dx_1} \quad \text{or} \quad J_{1r} = \frac{1}{3}x_{1r} = \frac{(GM_\odot)^{2/3}}{(18\dot{y}_{n1})^{1/3}}. \quad (6)$$

Since $A/H_K = O(M_n/M_\odot) \ll 1$ we expect $|\Delta J_1| \ll J_{1r}$, so we can expand H_K to second order in ΔJ_1 ; dropping unimportant constant terms the fast motion is determined by the Hamiltonian

$$\begin{aligned} H_f(\Delta J_1, w_1) &= \frac{9}{2} \left(\frac{d^2 H_K}{dx_1^2} \right)_{x_{1r}} (\Delta J_1)^2 + A(3J_{1r} + 3\Delta J_1, J_{1r} + \Delta J_1 + \frac{1}{3}J_2, w_1) \\ &= -\frac{27}{2a^2}(\Delta J_1)^2 + A(3J_{1r} + 3\Delta J_1, J_{1r} + \Delta J_1 + \frac{1}{3}J_2, w_1). \end{aligned} \quad (7)$$

The Hamiltonian is autonomous and hence has a conserved energy $E_f = H_f$ and action $I = (2\pi)^{-1} \oint \Delta J_1 dw_1$. The motion is along the level surfaces of H_f in the $(\Delta J_1, w_1)$ plane and typically consists of either libration (w_1 oscillates between fixed limits) or circulation (w_1 increases or decreases without reversing), just as in the case of the pendulum Hamiltonian. The stable equilibrium solutions (i.e. zero-amplitude libration) are given by

$$\Delta J_1 = \frac{a^2}{9} \left(\frac{\partial A}{\partial x_1} + \frac{1}{3} \frac{\partial A}{\partial x_2} \right), \quad \frac{\partial A}{\partial w_1} = 0, \quad \frac{\partial^2 A}{\partial w_1^2} < 0. \quad (8)$$

The slow motion is determined by averaging the Hamiltonian (4) over the fast motion:

$$H_s(J_2, w_2, t) = E_f(J_2) - \frac{1}{3}\dot{y}_{p2}J_2 + \langle B \rangle. \quad (9)$$

Here $\langle \cdot \rangle$ indicates an average over one period of the fast motion. The fast energy E_f depends on J_2 through the constraint that the fast action I is adiabatically invariant.

2.1. Solutions with zero-amplitude libration

The solutions to the fast and slow equations of motion are particularly simple in the case where the fast libration amplitude is zero for both Pluto and the Plutino. This approximation

is not particularly realistic—the libration amplitude of Pluto is 82° —but illustrates the principal features of the Plutino motions.

In this case the fast energy is

$$E_f = A(3J_{1r}, J_{1r} + \frac{1}{3}J_2, w_{1r}) \quad (10)$$

where w_{1r} is the equilibrium angle given by equation (8) and we have dropped much smaller terms that are $O(A^2)$. For simplicity we shall assume that there is only one stable equilibrium point, that is, one solution to equations (8) for given J_2 . At the equilibrium point the fast action is $I = 0$, and the slow Hamiltonian (9) is

$$H_s(J_2, w_2, t) = A(3J_{1r}, J_{1r} + \frac{1}{3}J_2, w_{1r}) - \frac{1}{3}\dot{y}_{p2}J_2 + \langle B(3J_{1r}, J_{1r} + \frac{1}{3}J_2, y_1, y_2, t) \rangle + O(A^2), \quad (11)$$

where $y_1 = \frac{1}{3}(w_{1r} + 2y_{n1} - y_2)$. Since Pluto also is assumed to have zero libration amplitude, $y_{p1} = \frac{1}{3}(w_{1r} + 2y_{n1} - y_{p2})$. Thus

$$3(y_{p1} - y_1) = y_2 - y_{p2} = 3w_2 \quad \text{mod } (2\pi); \quad (12)$$

that is, the difference in longitude of perihelion between Pluto and the Plutino is three times the difference in mean longitude. The same result will hold true on average even if the libration amplitudes are non-zero.

Now let us assume in addition that the eccentricities of both Pluto and the Plutino are small. Since their semi-major axes are the same, the gravitational potential from Pluto at the Plutino may be written

$$B = GM_p \left(\frac{\mathbf{r} \cdot \mathbf{r}_p}{|\mathbf{r}_p|^3} - \frac{1}{|\mathbf{r} - \mathbf{r}_p|} \right) = \frac{GM_p}{a} \left[\cos(y_1 - y_{p1}) - \frac{1}{2|\sin \frac{1}{2}(y_1 - y_{p1})|} \right]. \quad (13)$$

Using equation (12) this simplifies to

$$B = \frac{GM_p}{a} \left(\cos w_2 - \frac{1}{2|\sin \frac{1}{2}w_2|} \right). \quad (14)$$

Moreover

$$\frac{dy_{p2}}{dt} = \frac{\partial A}{\partial x_2}(3J_{1r}, J_{1r} + \frac{1}{3}J_2, w_{1r}) + O(A^2); \quad (15)$$

thus the slow Hamiltonian can be rewritten as

$$\begin{aligned} H_s(J_2, w_2) &= A(3J_{1r}, J_{1r} + \frac{1}{3}J_2, w_{1r}) - \frac{1}{3}J_2 \frac{\partial A}{\partial x_2}(3J_{1r}, J_{1r} + \frac{1}{3}J_2, w_{1r}) \\ &\quad + \frac{GM_p}{a} \left(\cos w_2 - \frac{1}{2|\sin \frac{1}{2}w_2|} \right) + O(A^2). \end{aligned} \quad (16)$$

The interesting behaviour occurs when the actions J_2 and J_{p2} are similar (i.e. the eccentricities of Pluto and the Plutino are similar), so we write $J_2 = J_{p2} + \Delta J_2$ and expand A to second order in ΔJ_2 . Dropping unimportant constants and terms of $O(A^2)$ we have

$$H_s(\Delta J_2, w_2) = \frac{1}{18} \Delta J_2^2 A_{22}(3J_{1r}, J_{1r} + \frac{1}{3}J_{p2}, w_{1r}) + \frac{GM_p}{a} \left(\cos w_2 - \frac{1}{2|\sin \frac{1}{2}w_2|} \right). \quad (17)$$

where $A_{22} = \partial^2 A / \partial x_2^2$.

This Hamiltonian is strongly reminiscent of the Hamiltonian for a test particle coorbiting with a satellite,

$$H_c(\Delta x, w) = -\frac{3}{2a^2} \Delta x^2 + \frac{GM}{a} \left(\cos w - \frac{1}{2|\sin \frac{1}{2}w|} \right); \quad (18)$$

here $\Delta x = x_1 - x_{s1}$ and $w = \lambda_1 - \lambda_{s1}$ are conjugate variables, and the subscript s denotes orbital elements of the satellite. In this case the torques from the satellite lead to changes in semi-major axis; for a Plutino the semi-major axis is locked to Neptune's by the resonance, so torques from Pluto lead to changes in the eccentricity instead.

When $A_{22} < 0$ many of the features of orbits in the slow Hamiltonian (17) follow immediately from the analogy with the Hamiltonian (18), which has been studied by many authors (e.g. Yoder et al. 1983, Namouni et al. 1999). The trajectories are determined by the level surfaces of the Hamiltonian. The equilibrium solutions correspond to the triangular Lagrange points in the coorbital case: $\Delta J_2 = 0$, $w_2 = \pm 60^\circ$, $H_s = -\frac{1}{2}GM_p/a$; the eccentricity of the Plutino equals the eccentricity of Pluto, the mean longitude leads or lags by 60° , and the perihelia are 180° apart. These solutions are maxima of the potential from Pluto. For smaller values of H_s , the orbits librate around the triangular points (“tadpole orbits”). Small-amplitude tadpole librations have frequency ω given by

$$\omega^2 = -\frac{1}{4} A_{22} \frac{GM_p}{a}. \quad (19)$$

The tadpole orbits merge at the separatrix orbit, $H_s = -\frac{3}{2}GM_p/a$; for this orbit the minimum separation is $w_{2,\min} = 23.91^\circ$. Even smaller values of H_s yield “horseshoe” orbits, with turning points at $\pm w_{2,\min}$ where $H_s = (GM_p/a)(\cos w_{2,\min} - \frac{1}{2}|\sin \frac{1}{2}w_{2,\min}|^{-1})$. For all tadpole and horseshoe orbits, the maximum and minimum values of ΔJ_2 occur at $w_2 = \pm 60^\circ$, and are given by

$$\Delta J_2 = \pm \left[\frac{18}{A_{22}} \left(H_s + \frac{GM_p}{2a} \right) \right]^{1/2}. \quad (20)$$

Eventually the theory breaks down, when $w_{2,\min}$ is small enough that adiabatic invariance is no longer a valid approximation.

2.2. The resonant potential from Neptune

For quantitative applications we must evaluate the resonant Neptune potential $A(\mathbf{x}, w_1)$. For small eccentricities, the potential can be derived analytically,

$$A(\mathbf{x}, w_1) = -\frac{GM_n}{a} \left[\frac{1}{2}b_{1/2}^{(0)}(\alpha) + \frac{1}{8}e^2(2\alpha D + \alpha^2 D^2)b_{1/2}^{(0)}(\alpha) + \frac{1}{2}e(5 + \alpha D)b_{1/2}^{(2)}(\alpha) \cos w_1 + \frac{1}{8}e^2(104 + 22\alpha D + \alpha^2 D^2)b_{1/2}^{(4)}(\alpha) \cos 2w_1 + O(e^3) \right], \quad (21)$$

where $\alpha = a_n/a < 1$, $D = d/d\alpha$,

$$b_{1/2}^{(j)}(\alpha) = \frac{1}{\pi} \int_0^{2\pi} \frac{d\phi \cos j\phi}{(1 - 2\alpha \cos \phi + \alpha^2)^{1/2}} \quad (22)$$

is a Laplace coefficient, Neptune is assumed to be on a circular orbit, and inclinations are neglected.

Unfortunately, in the present case the high eccentricity of the Plutino orbits makes this expansion invalid. However, we may determine $A(\mathbf{x}, w_1)$ numerically for given actions \mathbf{x} by averaging the gravitational potential from Neptune over y_2 at fixed w_1 , that is,

$$A(\mathbf{x}, w_1) = -\frac{GM_n}{a} F(\mathbf{x}, w_1), \quad (23)$$

where

$$F(\mathbf{x}, w_1) = \frac{a}{6\pi} \int_0^{6\pi} dy_2 \left(\frac{1}{|\mathbf{r}_n - \mathbf{r}|} - \frac{\mathbf{r} \cdot \mathbf{r}_n}{|\mathbf{r}_n|^3} \right)_{\mathbf{x}, w_1, y_2} + \text{constant}; \quad (24)$$

the unimportant constant is chosen so that $A = 0$ for circular orbits, i.e. $F(x_1, 0, w_1) = 0$. It can be shown analytically that the contribution from the second (indirect) term in the integrand vanishes.

We shall also write

$$A_{22} = \frac{\partial^2 A}{\partial x_2^2} \equiv -\frac{M_n}{M_\odot a^2} F_{22}(\mathbf{x}, w_1) \quad \text{where} \quad F_{22}(\mathbf{x}, w_1) = x_1^2 \frac{\partial^2 F(\mathbf{x}, w_1)}{\partial x_2^2}. \quad (25)$$

Figure 1 plots the contours of $F(\mathbf{x}, w_1)$ at the resonant semimajor axis x_{1r} , as obtained from equation (24). The potential is singular for collision orbits, which for small eccentricity satisfy

$$\cos w_1 = \frac{a - a_n}{ea}. \quad (26)$$

The conditions (8) for stable zero-amplitude libration are satisfied if and only if $w_1 = w_{1r} = \pi$ or $w_1 = 0$ and $e > 1 - a_n/a = 0.237$. Figure 2 and 3 show examples of these two solutions,

plotted in a reference frame corotating with Neptune. Orbits of the first kind are similar to Pluto’s, although with smaller libration amplitude (compare Fig. 4 of Malhotra & Williams 1997). Orbits of the second kind (Fig. 3) were discussed by Malhotra (1996), who calls them “perihelion librators”. We shall not discuss these further, since they do not appear to form naturally during resonance capture of initially circular orbits; moreover for $e \gtrsim 0.35$ they are likely to be unstable, since they cross Uranus’s orbit and thus are subject to close encounters and collisions with that planet.

Figure 4 plots $F(x_{1r}, x_2, \pi)$ and $F_{22}(x_{1r}, x_2, \pi)$; at the eccentricity of Pluto, corresponding to $x_2/(GM_{\odot}a)^{1/2} = 0.0325$, we have $F(x_{1r}, x_2, \pi) = -0.313$ and $F_{22}(x_{1r}, x_2, \pi) = 79.3$. Thus, for example, the eccentricity oscillation in the separatrix orbit that marks the boundary between tadpole and horseshoe orbits has amplitude $\Delta e = 0.007$ (eq. 20) and the period of libration of small tadpole orbits is $2\pi/\omega = 9.1 \times 10^7$ yr (eq. 19).

For our purposes it is sufficient to work with the following numerical approximation to the resonant potential:

$$\tilde{F}(\mathbf{x}, w_1) = -\frac{0.584 + 0.130e}{1 + 1.709e} \ln |1 - 4.222e \cos w_1|, \quad (27)$$

where $x_2 = x_{1r}[1 - (1 - e^2)^{1/2}]$. This approximation is chosen to match the resonant potential at the resonant semimajor axis $x_1 = x_{1r}$; the dependence on the relative semimajor axes of Neptune and the Plutino is suppressed since the effects of this potential are only important near resonance. The logarithmic factor is chosen to reproduce the singularity in the resonant potential near the collision orbits defined approximately by equation (26). The approximation formula also matches the analytic formula (21) to $O(e^2)$ at $w_1 = \pi$.

Figure 5 shows the contour plot analogous to Figure 5 for the approximate resonant potential \tilde{F} , and the triangles in Figure 4 show \tilde{F} and \tilde{F}_{22} . The agreement is very good, especially considering that errors are amplified by taking the two derivatives required to generate \tilde{F}_{22} .

3. Numerical experiments

We follow the orbital evolution of Pluto and a Plutino in a simplified version of the Sun-Neptune-Pluto-Plutino four-body system that isolates the resonant potential from Neptune. Neptune is assumed to have a circular orbit that migrates outward according to the rule (Malhotra 1993)

$$a_n(t) = a_f - \Delta a \exp(-t/\tau), \quad (28)$$

where $a_f = 30.17$ AU is Neptune’s present semimajor axis, $\Delta a = 6$ AU, and $\tau = 1.5$ Myr. Thus Neptune’s initial semimajor axis is 24.17 AU and the initial location of the 3:2 orbital resonance is 31.67 AU.

The initial eccentricity of Pluto is taken to be zero and its initial semimajor axis is 33 AU, as required so that its present eccentricity matches the observed value (eq. 5). We followed 160 test particles, with initial semimajor axes distributed uniformly in the range [31 AU, 39 AU] and eccentricities distributed uniformly in the range [0, 0.03]. The inclinations of Pluto and the test particles are chosen randomly in the range $[0, 3^\circ]$ and their angular elements are chosen randomly from $[0, 2\pi]$. Pluto and the test particles feel the resonant potential from Neptune, as defined by equations (23) and (27), but no other Neptune forces. The effects of the resonant Neptune potential on the orbital elements of Pluto and the test particles are followed using Lagrange’s equations.

The test particles do not influence Pluto or one another. However, they are subject to the gravitational potential from Pluto,

$$B(\mathbf{x}, \mathbf{y}, t) = -GM_p \left(\frac{1}{|\mathbf{r} - \mathbf{r}_p|} - \frac{\mathbf{r} \cdot \mathbf{r}_p}{|\mathbf{r}_p|^3} \right); \quad (29)$$

the effects of this potential on the orbital elements of the test particles are followed using Gauss’s equations.

The evolution of Pluto and the test particles is followed for 0.45 Gyr or 10% of the age of the solar system.

4. Results

Of the 160 test particles, all but 12 are captured into the 3:2 resonance with Neptune, in the sense that their final semimajor axes are close to $(3/2)^{2/3}a_n$ and their eccentricities are near the prediction of equation (5), as shown in Figure 6. The 12 particles that are not captured lie inside the location of Neptune’s 3:2 resonance at the start of the calculation, $(3/2)^{2/3} \times 24.17$ AU = 31.67 AU, and would presumably be captured into other resonances if we used the full Neptune potential to work out their motion. We have verified this presumption by conducting shorter integrations (1×10^7 yr) using the same initial conditions but the complete Neptune potential. In this case all but 15 of the 160 particles were captured into the 3:2 resonance; the remainder were captured into the 4:3, 5:3 or 7:5 resonances.

The behavior of the test particles in the 3:2 resonance (henceforth Plutinos) falls into the following broad classes:

- Tadpole orbits (5 particles): these have longitude difference $y_1 - y_{p1}$ and differences in longitude of perihelion $y_{p2} - y_2$ that librate around the leading or trailing Lagrange point of Pluto (Figure 7). (Note that the libration center for the orbit in this Figure is $y_1 - y_{p1} \simeq 100^\circ$, not 60° as implied by the analysis in §2.1. This discrepancy arises because Pluto has a high eccentricity, while our analysis is only valid for near-circular orbits. Similarly, the perihelion difference librates around $\varpi - \varpi_p \simeq 300^\circ$, three times the difference in mean longitude as required by eq. 12.) The tadpoles show no evidence of chaotic behavior or secular evolution over the length of our integration. The analysis in §2.2 suggests that the maximum eccentricity difference for these orbits is $\Delta e \simeq 0.007$; this requires in turn that their initial semimajor axes must have been close to Pluto’s, as is seen to be the case in Figure 6.
- Horseshoe orbits (19 particles): the longitude difference oscillates around 180° , with jumps in the Plutino eccentricity at the extrema of the longitude oscillation, as predicted by the analysis of §2.1 (Figures 8, 9). The motion appears stable over the length of our integration although there are significant variations in semimajor axis oscillations during the course of the integration, and some horseshoes may evolve into transitional orbits over longer time intervals.
- Transitional orbits (43 particles): these show irregular behavior or transitions between libration and circulation of the longitude difference (Figure 10). When the longitude difference circulates, the particles are no longer protected from close encounters with Pluto. However, the particles remain in the 3:2 Neptune resonance in the sense that the resonant angle w_1 continues to librate.
- Doubly transitional orbits (2 particles): Like transitional orbits, these show libration-circulation transitions in the longitude difference, but in addition they show irregular behavior in the resonant angle w_1 , leading eventually to a transition of w_1 from libration to circulation (Figure 11). Although only 2 particles in our simulation exhibit this behavior, a number of others show growing amplitude in the w_1 libration and will probably move into this class in less than the age of the solar system. Such orbits are normally short-lived since once w_1 circulates, they are no longer protected from close encounters with Neptune.
- Irregular circulating orbits (17 particles): the longitude difference circulates throughout the integration. Pluto induces irregular behavior (Figure 12), but the Neptune resonance is preserved in the sense that w_1 continues to librate, at least over the span of our integration.
- Regular circulating orbits (62 particles): the longitude difference circulates throughout

the integration, but the orbits appear fairly regular (Figure 13). Generally, the orbits with larger eccentricity differences are more regular, because the encounter velocity with Pluto is higher so the perturbations from close encounters are smaller.

These classes represent a sequence in eccentricity difference: the typical eccentricity difference $|e - e_p|$ is smallest for tadpoles and largest for orbits unaffected by Pluto. Because the Plutino eccentricity is determined by the semimajor axis at the time of resonant capture (eq. 5), the classes also reflect the initial semimajor axes of the Plutinos: the tadpoles and horseshoes all have initial semimajor axes in the range 32.2 AU–34.2 AU (i.e. close to Pluto’s initial semimajor axis of 33 AU). The transitional and irregular circulating Plutinos mostly have initial semimajor axes in the range 31.7 AU–36 AU, and the regular circulating Plutinos have initial semimajor axes concentrated in the range 35 AU–39 AU.

5. Discussion

Test particles captured into the 3:2 Neptune resonance (Plutinos) have a complex range of dynamical interactions with Pluto. The strength of the interaction depends on the difference in eccentricity between the test particle and Pluto, and thus on the difference in initial semi-major axis if the initial orbits were circular and capture occurred through outward migration of Neptune. Plutinos are stable only if the eccentricity difference Δe is small ($\Delta e \lesssim 0.02$ from Figure 6), in which case the Plutinos librate on tadpole or horseshoe orbits; or if the eccentricity difference is large ($\Delta e \gtrsim 0.06$), in which case the longitude difference circulates but relative velocity at encounter is high enough that Pluto has little effect. Unstable orbits at intermediate Δe can be driven out of the 3:2 Neptune resonance by interactions with Pluto, and thereafter are short-lived because of close encounters with Neptune. Thus we expect that the population of Plutinos has decayed over time, although determining the survival fraction will require integrations over the lifetime of the solar system using the full Neptune potential.

The long-term behavior of orbits in the 3:2 Neptune resonance is central to the origin of Jupiter-family comets. The usual explanation is that slow chaotic diffusion and collisional kicks drive Plutinos out of the 3:2 resonance, after which they are subjected to close encounters with the giant planets and eventually evolve into Jupiter-family comets (Morbidelli 1997). Our results suggest that Pluto-induced evolution of Plutinos onto Neptune-crossing orbits may contribute to or even dominate the flux of Jupiter-family comets.

Our results also enhance the motivation to obtain accurate orbits for Kuiper-belt objects, and fuel speculation that the formation of the Pluto-Charon binary may be linked to

interactions between Pluto and Plutinos.

This research was supported in part by NASA Grant NAG5-7310. We thank Matt Holman, Renu Malhotra, and Fathi Namouni for discussions and advice.

REFERENCES

- Cohen, C. J., & Hubbard, E. C. 1965, *AJ*, 70, 10
- Fernández, J. A., & Ip, W.-H. 1984, *Icarus*, 58, 109
- Malhotra, R. 1993, *Nature*, 365, 819
- Malhotra, R. 1995, *AJ*, 110, 420
- Malhotra, R. 1996, *AJ*, 111, 504
- Malhotra, R. 1998, 29th Annual Lunar and Planetary Science Conference, Houston, TX, abstract no. 1476
- Malhotra, R., & Williams, J. G. 1997, in *Pluto and Charon*, eds. S. A. Stern and D. J. Tholen (Tucson: University of Arizona Press), 127
- Malhotra, R., Duncan, M., & Levison, H. 1999, in *Protostars and Planets IV*.
- Morbidelli, A. 1997, *Icarus*, 127, 1
- Namouni, F., Christou, A. A., & Murray, C. D. 1999, astro-ph/9904016
- Stern, S. A. 1992, *ARAA*, 30, 185
- Tholen, D. J., & Buie, M. W. 1997, in *Pluto and Charon*, eds. S. A. Stern and D. J. Tholen (Tucson: University of Arizona Press), 193
- Yoder, C. F., Colombo, G., Synnott, S. P., & Yoder, K. A. 1983, *Icarus*, 53, 431

Fig. 1.— A contour plot of the resonant gravitational potential $F(\mathbf{x}, w_1)$ at the resonant semimajor axis, $x_1 = x_{1r}$ (eq. 6), as obtained from equation (24). The ordinate is eccentricity, which is a proxy for $x_2 = x_{1r}[1 - (1 - e^2)^{1/2}]$. The contour levels are uniformly spaced at intervals of 0.01; positive contours are solid and negative contours are dotted.

Fig. 2.— The orbit of a Plutino for 20,000 years in a reference frame corotating with Neptune. Initially the resonant angle $w_1 = 180^\circ$ and the eccentricity $e = 0.39$. The high eccentricity was chosen to illustrate the character of the orbit; in a more realistic integration this orbit would be unstable because it crosses the orbit of Uranus.

Fig. 3.— The orbit of a Plutino for 20,000 years in a reference frame corotating with Neptune. Initially the resonant angle $w_1 = 0^\circ$ and $e = 0.49$. In a more realistic integration this orbit would be unstable, since it crosses the orbit of Uranus.

Fig. 4.— The solid curves plot $F(x_{1r}, x_2, \pi)$ and $(x_2/x_{1r})^{3/2}F_{22}(x_{1r}, x_2, \pi)$ as determined by the numerical integral (24) and equation (25) (the multiplicative factor in front of F_{22} is used because $F_{22} \propto x_2^{3/2}$ as $x_2 \rightarrow 0$). The solid triangles and dashed line show the approximations \tilde{F} and \tilde{F}_{22} given by equation (27). For reference, the eccentricity of Pluto, $e = 0.253$, is marked by an open circle at $x_2/(GM_\odot a)^{1/2} = 0.0325$.

Fig. 5.— The contour graph of the approximation \tilde{F} (eq. 27) to the resonant gravitational potential. The contour levels are the same as in Figure 1.

Fig. 6.— The final eccentricity of the test particles as a function of their initial semimajor axis. The solid curve is the prediction of equation (5), and the crossing point of the dashed lines shows the location of Pluto, computed with the same equation. The symbols denote the orbit classes discussed in §4: tadpole orbits (open circles), horseshoe orbits (solid circles), transitional orbits (crosses), doubly transitional orbits (open squares), irregular circulating orbits (starred squares), regular circulating orbits (solid triangles), orbits not captured into the 3:2 resonance (open triangles).

Fig. 7.— A tadpole orbit. In the first panel “dpp” denotes the distance between Pluto and the Plutino in AU. Subsequent panels show longitude of perihelion, mean longitude, semimajor axis, eccentricity, orbital period ratio to Neptune, and the resonant angle of the Plutino; the detailed definitions of the orbital elements are in the text.

Fig. 8.— A horseshoe orbit.

Fig. 9.— A second horseshoe orbit. The spikes in $\lambda - \lambda_p$ arise because small short-period oscillations occasionally carry this angle past 0 or 2π .

Fig. 10.— A transitional orbit.

Fig. 11.— A doubly transitional orbit.

Fig. 12.— An irregular circulating orbit.

Fig. 13.— A regular circulating orbit.

This figure "fig1.gif" is available in "gif" format from:

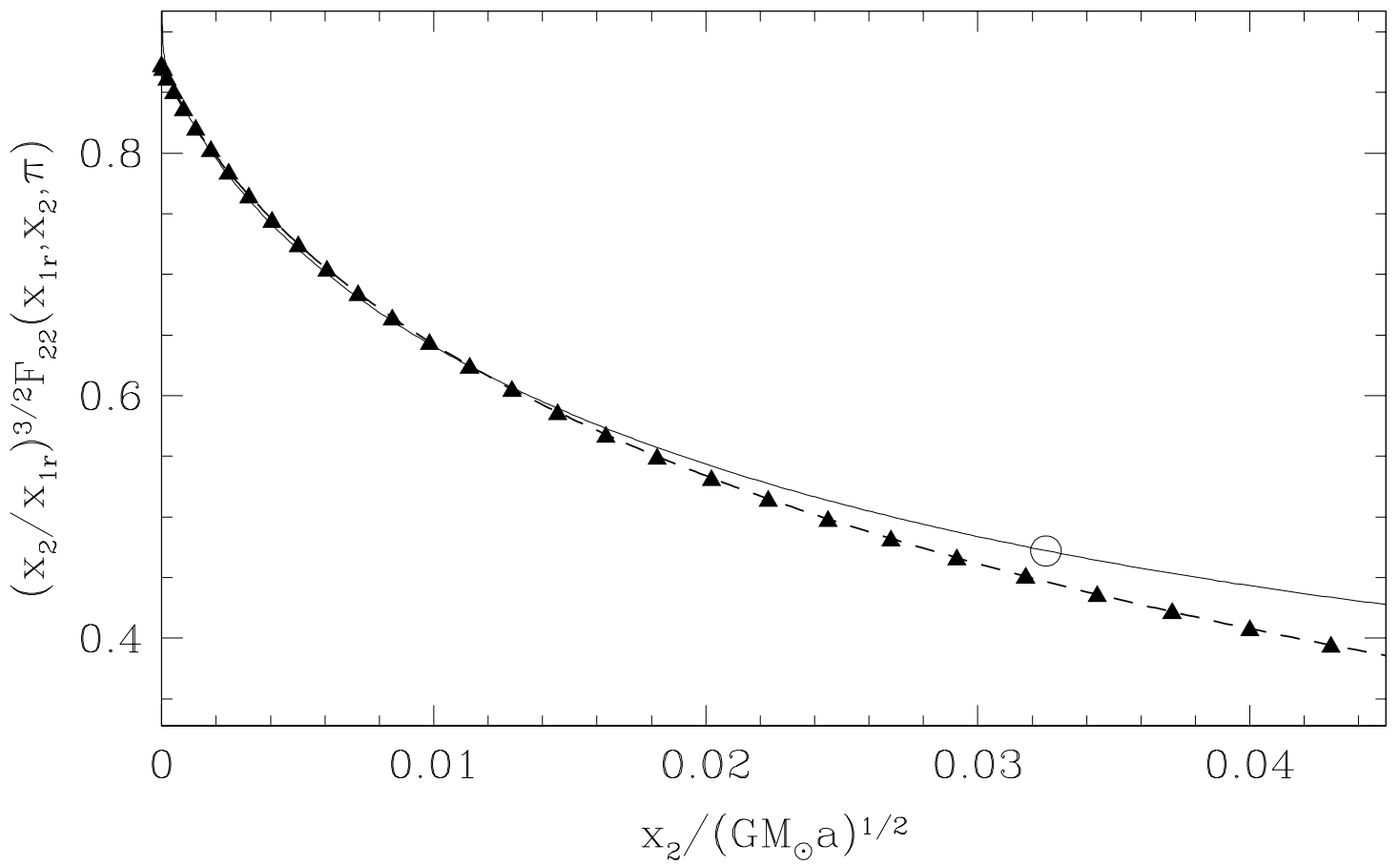
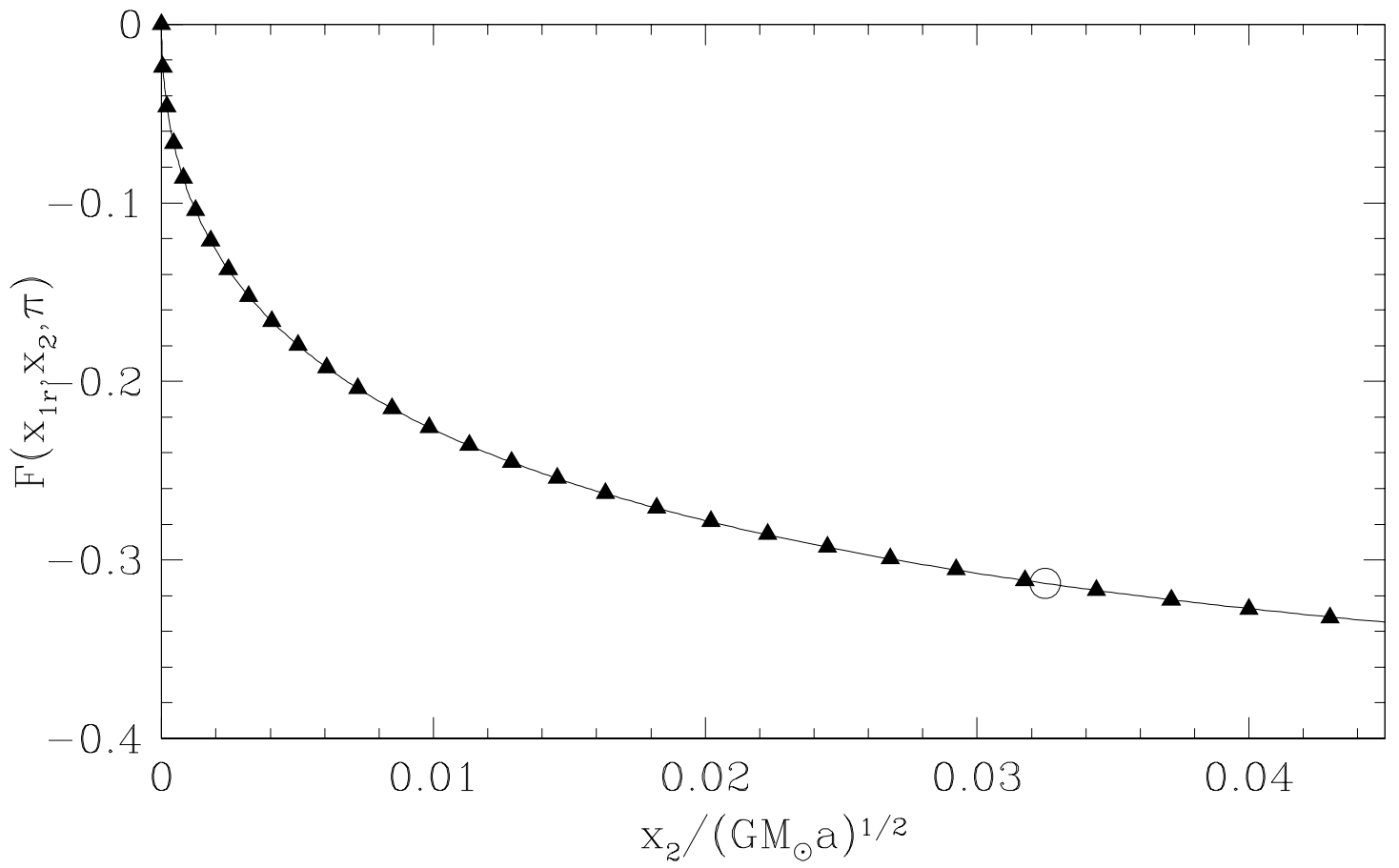
<http://arxiv.org/ps/astro-ph/9904424v1>

This figure "fig2.gif" is available in "gif" format from:

<http://arxiv.org/ps/astro-ph/9904424v1>

This figure "fig3.gif" is available in "gif" format from:

<http://arxiv.org/ps/astro-ph/9904424v1>



This figure "fig5.gif" is available in "gif" format from:

<http://arxiv.org/ps/astro-ph/9904424v1>

